

# Reversible Scrolling of Two-Dimensional Sheets from the Self-Assembly of Laterally Grafted Amphiphilic Rods\*\*

Eunji Lee, Jung-Keun Kim, and Myongsoo Lee\*

Hollow tubular structures have attracted much attention owing to their unique optoelectrical properties and potential applications in biomimetics, nanodevices, catalysis, and energy storage.<sup>[1]</sup> Since the discovery of carbon nanotubes,<sup>[2]</sup> extensive efforts have been devoted to experimentally fabricate organic nanotubes in aqueous solutions, and theoretically understand the aspects of nanotube formation. For example, introduction of a chiral moiety into aromatic amphiphilic molecular architectures leads to the initial formation of helical ribbons, which in turn, self-assemble into nanotubes.<sup>[3]</sup> It is known that ring-shaped, flat cyclic peptides composed of an even number of alternating D- and L-amino acids stack on top of each other through intermolecular hydrogen bonding to form nanotubes.<sup>[4]</sup> Despite the above achievements, the development of a novel route for nanotube formation is still a challenging field of research.

Theoretical studies have predicted that two-dimensional (2D) anisotropic sheets with long-range orientational order might exhibit a tubular phase, which is intermediate in its properties and location on the phase diagram between a flat low-temperature phase and a crumpled high-temperature phase.<sup>[5]</sup> In this tubular phase, the sheets begin to curl in one direction as thermal stress increases the bending of the sheets in a preferential direction, stabilizing orientational order against the thermal stresses. Inspired by this theoretical prediction, we envisioned that the transformation of sheetlike structure into tubular structure would be experimentally feasible if the introduction of a laterally extended aromatic rodlike scaffold into amphiphilic molecules can lead to the formation of in-plane anisotropic sheets.<sup>[6]</sup> Therefore, we designed laterally grafted rod amphiphiles consisting of a hepta(*p*-phenylene) rod in which hydrophilic oligoether dendrons and hydrophobic branched heptyl chains are grafted opposite to each other at the midpoint of the rodlike scaffold (**1** and **2**).

Herein, we report the spontaneous formation of a sheetlike structure, which is based on the 2D self-assembly of

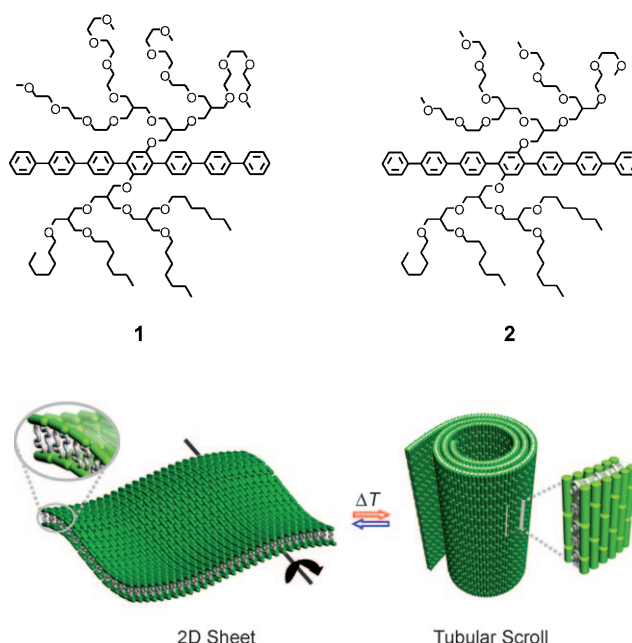


**Figure 1.** Representation of reversible scrolling of anisotropic planar sheets.

rationally designed rod amphiphiles. These sheets undergo reversible transformation into tubular scrolls upon heating (Figure 1). The synthesis of the laterally grafted amphiphilic rod molecules was performed with the preparation of oligoether dendrons and branched alkyl chains according to the procedure described previously.<sup>[7,8]</sup> The ter(*p*-phenylene) aromatic scaffold was prepared using the Suzuki coupling reaction with 1,4-dibromo-2,5-dimethoxybenzene and a boronic acid derivative followed by iodination. The final rod amphiphiles were synthesized by etherification of the aromatic scaffold and tosylation of the oligoether dendrons and branched alkyl chains, and thereafter the Suzuki coupling reaction with the biphenyl units. The analytical data from the resulting molecules **1** and **2** are in full agreement with the expected chemical structures.<sup>[9]</sup>

The aggregation behavior of the laterally grafted amphiphilic rod molecules was studied in aqueous solution (0.01 wt %) using fluorescence spectroscopy. The intensity of the fluorescence maxima was quenched with respect to that observed in chloroform, indicating the aggregation of aromatic segments (Figure 2a and Supporting Information, Figure S2).<sup>[10]</sup> Dynamic light scattering (DLS) experiments were performed on the amphiphiles in aqueous solution (0.01 wt %) to further investigate the aggregation behavior.<sup>[11]</sup> The relaxation times obtained for these amphiphiles in an aqueous

[\*] E. Lee, J.-K. Kim, Prof. M. Lee  
Center for Supramolecular Nanoassembly and  
Department of Chemistry, Yonsei University  
Shinchon 134, Seoul 120-749 (Korea)  
Fax: (+82) 2-393-6096  
E-mail: mslee@yonsei.ac.kr  
Homepage: <http://csna.yonsei.ac.kr>

[\*\*] This work was supported by the National Creative Research Initiative Program of the Korean Ministry of Science and Technology. E.L. and J.-K.K. acknowledge a fellowship of the BK21 program from the Ministry of Education and Human Resources Development.

Supporting information for this article is available on the WWW under <http://dx.doi.org/10.1002/ange.200900079>.

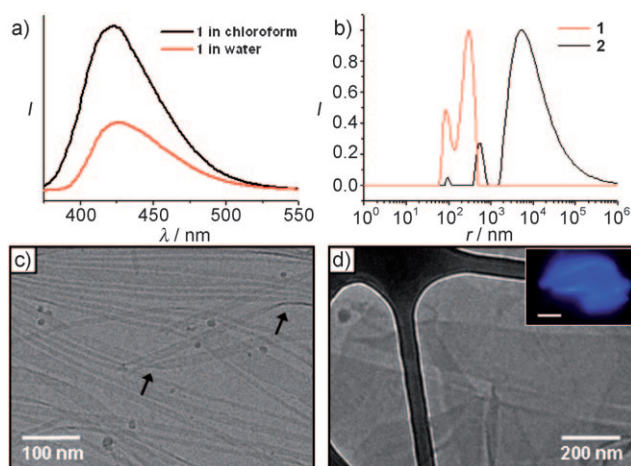


**Figure 2.** a) Fluorescence emission spectra of **1** (0.01 wt%) in water (red) and chloroform (black). The excitation wavelength is  $\lambda_{\text{ex}} = 293$  nm. b) Size distribution graphs of **1** and **2** in aqueous solution at a scattering angle of  $90^\circ$ . Cryo-TEM images showing c) the flat ribbons of **1** (arrows indicate folded edge of ribbons) and d) the wrinkled sheets of **2** in aqueous solution (inset: fluorescence micrograph in aqueous solution, scale bar:  $2\ \mu\text{m}$ ).

solution of **1** using the correlation function is shorter than that of **2** (Supporting Information, Figure S3). The CONTIN analysis of autocorrelation function for both solutions showed that **2** formed large aggregates with much broader distributions compared to **1** (Figure 2b).

Cryogenic transmission electron microscope (cryo-TEM) has been performed with the 0.01 wt % aqueous solutions of **1** and **2** to further confirm the structure of the aggregates. The images of **1**, which is based on tri(ethylene oxide) chains, showed dark ribbonlike aggregates with various widths against the vitrified solution background (Figure 2c). Close examination of the objects revealed folded edges of individual aggregates with a thickness of approximately 4 nm. The hydrophobic cores have a darker appearance; however, the solvated oligoether dendrons remained invisible.<sup>[8a,12]</sup> Therefore, the dimension of the individual aggregates is in reasonable agreement with twice the length of the hydrophobic segments including the aromatic segments and alkyl chains (ca. 2.3 nm by CPK modeling), thus confirming the bilayer packing.<sup>[13]</sup> Based on these results, it can be concluded that **1** self-assembles into a flat ribbon structure in which the rods are arranged parallel to the ribbon plane.

The formation of a ribbonlike structure of **1** led us to investigate whether decreasing the oligoether chain length leads to the system assuming larger 2D aggregates to reduce the exposure of the ribbon edges to water molecules. With this in mind, we have prepared rod amphiphile **2** based on short di(ethylene oxide) chains. As expected, the fluorescence microscopy image of **2** (0.01 wt % aqueous solution) revealed the presence of large sheets (Figure 2d, inset). Also, the magnification of the 2D objects by cryo-TEM showed the crumpled sheets ranging in size from several hundreds to a few micrometers (Figure 2d). However, in the some cases, flat sheets that are not wrinkled were also observed (Supporting Information, Figure S4). For cryo-TEM experiments, samples

were prepared by suspending 100–200 nm thickness film of the 0.01 wt % solutions on a lacey TEM grid, which was then plunged into liquid ethane to freeze the solution containing the aggregates. Thus, the large wrinkled sheets in the observed TEM image were assumed to be induced by specimen preparation. The formation of flat sheetlike structures was further confirmed by atomic force microscopy (AFM). An AFM investigation of **2** showed planar sheets with a uniform thickness of about 5.4 nm, which indicates that the amphiphiles of **2** are also packed in a bilayer arrangement (Supporting Information, Figure S5). These results demonstrate that a decrease of hydrophilic chains in length enhances the aggregation of the laterally extended aromatic amphiphiles and thereby transformation of the ribbons into 2D sheets.

Notably, the aqueous solutions of **1** and **2** were shown to reversibly transform from transparent to translucent states at about  $45^\circ\text{C}$  owing to lower critical solution temperature (LCST) of the oligoether dendrons (Supporting Information, Figure S6).<sup>[8,14]</sup> To corroborate thermoresponsive structural change at the LCST, cryo-TEM was carried out with both samples as a function of temperature. When the temperature was raised to  $60^\circ\text{C}$ , cryo-TEM images of **1** showed a sheetlike structure, indicating that the ribbons transform into a 2D sheet structure upon heating (Figure 3a). An AFM image of the same sample showed that the thickness of the sheets is circa 5.9 nm, which is indicative of a bilayer (Figure 3b).

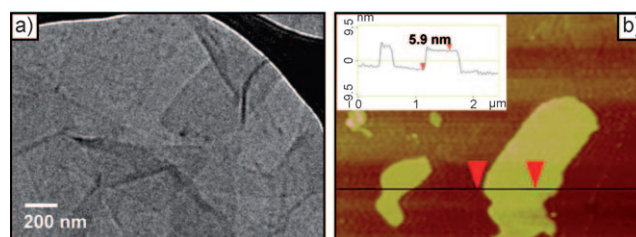


**Figure 3.** a) Cryo-TEM image, and b) AFM image (inset: height profile along black line) of an aqueous solution of **1** (0.01 wt %) at  $60^\circ\text{C}$ .

Above the LCST, the oligoether dendritic chains are dehydrated and can assemble into molecular globules, which can lead to a decrease in the effective hydrophilic volume, resulting in the exposure of the hydrophobic side faces of the ribbons to water. To reduce this unfavorable interaction, the ribbons were associated through side-by-side hydrophobic interactions to form a 2D sheet. This finding is reflected in the increased fluorescence quenching with increasing temperature, which implies that the aromatic segments are packed more closely within the core because of the increase in hydrophobic environments caused by dehydration of oligoether dendritic chains (Supporting Information, Figure S7).

Remarkably, the planar sheets of **2** roll up into tubular scrolls upon heating to the LCST. In contrast to the image taken at room temperature, the fluorescence micrograph taken at  $60^\circ\text{C}$  revealed the formation of elongated rodlike assemblies (Figure 4a). Some of the objects do not look like elongated rods owing to their continuous Brownian motion,

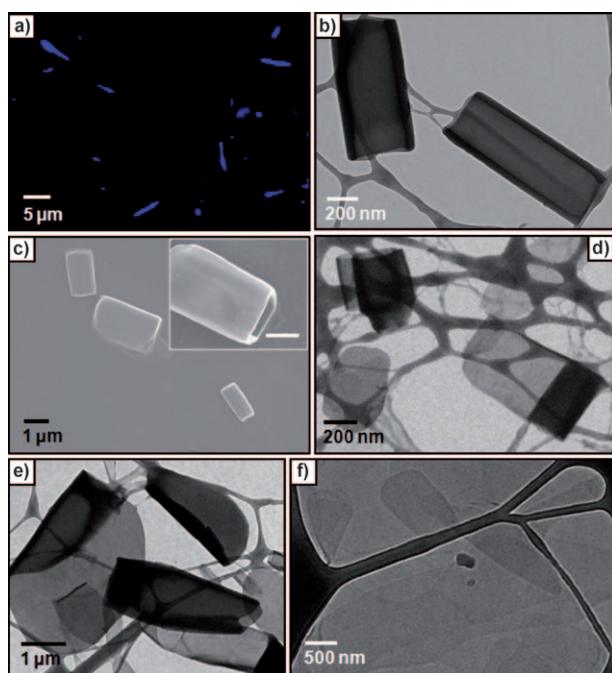


**Figure 4.** a) Fluorescence, b) cryo-TEM, and c) SEM micrographs in aqueous solution of **2** at 60°C; scale bar in the inset: 500 nm. d) TEM images of aqueous solution of **2** (0.01 wt%) at 45°C. After heating to 60°C, the solution of **2** was slowly cooled to room temperature and allowed to age for e) 12 h and f) 2 weeks as the tubular scrolls regenerate into unfolded sheets.

although they are tubular in shape. For direct visualization of the rodlike objects formed in aqueous solution, cryo-TEM experiments were performed with a 0.01 wt% aqueous solution of **2**. The images show a hollow tubular structure, demonstrating that the tubular objects are formed in bulk solution (Figure 4b and Supporting Information, Figure S8). However, the presence of large tubular particles of sizes greater than the thickness of the freely suspended film is not enough to provide the obvious differences in electron density that are required to distinguish the structures. Thus, to obtain the structural information, the frozen specimens were slightly defrosted, although the transformation into tubular objects was confirmed by scanning electron microscopy (SEM). The SEM images clearly showed short tubular objects with a hollow interior (Figure 4c and Supporting Information, Figure S8), which is consistent with the results obtained from fluorescence microscopy and TEM. To understand the formation mechanism of the tubular structure, TEM experiments were performed at different temperatures. Upon heating to 45°C, TEM micrographs of the solution show the loosely rolled sheets (Figure 4d). On further heating to 60°C, we observed closed tubular scrolls (Figure 4b and Supporting Information, Figure S8). After annealing at room temperature for 12 h, the tubular scrolls opened into sheets (Figure 4e). Complete recovery to the original sheets took place over a period of two weeks upon resting at room temperature (Figure 4f), indicating that the structural transformation between tubular scrolls and planar sheets occurs in a reversible way.

Spontaneous scrolling of the planar sheets upon heating is attributed again to a LCST behavior of the oligoether chains located at the planar surface. Above the LCST, the planar sheets, where the rod segments are aligned parallel to the sheet plane, would be unstable owing to the enhanced surface energies arising from the increase in hydrophobicity of the oligoether chains as a result of dehydration. To reduce unfavorable contact between hydrophobic surfaces and water, the planar sheets roll up along the direction of the rod to form tubular scrolls (Figure 1).

The preservation of the large planar sheets at room temperature can be attributed to a strong tendency of the rod segments to efficiently pack with an anisotropic arrangement through strong  $\pi$ - $\pi$  stacking interactions. Thus, we envisioned that the intercalation of the hydrophobic dye molecules between the aromatic segments in the sheets would frustrate the aromatic interactions and subsequently drive the sheets to roll up into tubular scrolls to reduce the penalty in energy associated with the packing frustration of the rod segments within the aromatic cores. To show this frustrated interaction, the intercalation experiments of **2** have been performed with hydrophobic dye, Nile Red. The intercalation of Nile Red within the aromatic segments was confirmed by fluorescence spectroscopy (Figure 5a). When the solution **2** containing the

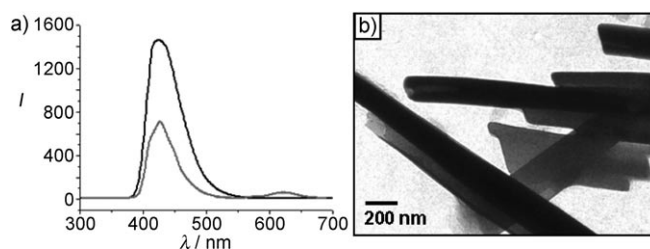


**Figure 5.** a) Emission spectra of a solution (black) of **2** (0.01 wt%) and a mixture (gray) of **2** (0.01 wt%) and Nile Red (0.001 wt%). The excitation wavelength is  $\lambda_{\text{ex}} = 293$  nm. b) TEM image showing the scroll-type tubes of **2** containing 10 mol% Nile red without staining (0.01 wt%).

Nile Red was excited at 293 nm, the fluorescence intensity of **2** was suppressed while exhibiting strong emission at 620 nm corresponding to the energy-transfer band of the Nile Red dye. These emission bands clearly indicate the intercalation of Nile Red within the rod segments.<sup>[15]</sup> Indeed, TEM image showed that **2** containing Nile Red forms tubular scrolls (Figure 5b). The fluorescence and the TEM results indicate that the in-plane anisotropic sheets have a strong tendency to form scroll-type tubes by reducing the surface energy against external stress.

In most of the cases of self-assembling systems including block copolymers and surfactant molecules, the 2D sheets fold into hollow spheres.<sup>[16]</sup> Thus, a remarkable feature of our system is the ability of the 2D sheets to roll up into hollow tubules. This unique structural transformation arises from in-plane orientational order of the rod segments in which the rods are arranged parallel to the sheet plane.<sup>[5]</sup> The resulting anisotropic sheets, upon heating, spontaneously roll up along the direction of the rod axis to form tubular scrolls. Thus the



design of rod amphiphiles with lateral chains provides a novel opportunity to construct hollow 1D nano-objects.

Received: January 6, 2009

Published online: April 16, 2009

**Keywords:** amphiphiles · anisotropic sheets · nanotubes · rod-coil assemblies · self-assembly

- [1] a) C. R. Martin, P. Kohli, *Nat. Rev. Drug Discovery* **2003**, 2, 29–37; b) J. P. Hill, W. Jin, A. Kosaka, T. Fukushima, H. Ichihara, T. Shimomura, K. Ito, T. Hashizume, N. Ishii, T. Aida, *Science* **2004**, 304, 1481–1483; c) M. A. Balbo Block, S. Hecht, *Angew. Chem.* **2005**, 117, 7146–7149; *Angew. Chem. Int. Ed.* **2005**, 44, 6986–6989; d) T. Shimizu, M. Masuda, H. Minamikawa, *Chem. Rev.* **2005**, 105, 1401–1443.
- [2] S. Iijima, *Nature* **1991**, 354, 56–58.
- [3] W.-Y. Yang, E. Lee, M. Lee, *J. Am. Chem. Soc.* **2006**, 128, 3484–3485.
- [4] a) M. R. Ghadiri, J. R. Granja, R. A. Milligan, D. E. McRee, N. Khazanovich, *Nature* **1993**, 366, 324–327; b) J. D. Hartgerink, J. R. Granja, R. A. Milligan, M. R. Ghadiri, *J. Am. Chem. Soc.* **1996**, 118, 43–50.
- [5] a) L. Radzihovsky, J. Toner, *Phys. Rev. Lett.* **1995**, 75, 4752–4755; b) M. Bowick, M. Falcioni, G. Thorleifsson, *Phys. Rev. Lett.* **1997**, 79, 885–888.
- [6] C. Tschierske, *Chem. Soc. Rev.* **2007**, 36, 1930–1970.
- [7] J.-K. Kim, E. Lee, Y.-H. Jeong, J.-K. Lee, W.-C. Zin, M. Lee, *J. Am. Chem. Soc.* **2007**, 129, 6082–6083.
- [8] a) J.-K. Kim, E. Lee, Y.-b. Lim, M. Lee, *Angew. Chem.* **2008**, 120, 4740–4744; *Angew. Chem. Int. Ed.* **2008**, 47, 4662–4666; b) E. Lee, Y.-H. Jeong, J.-K. Kim, M. Lee, *Macromolecules* **2007**, 40, 8355–8360.
- [9] See the Supporting Information.
- [10] a) A. P. H. J. Schenning, P. Jonkhøj, E. Peeters, E. W. Meijer, *J. Am. Chem. Soc.* **2001**, 123, 409–416; b) A. P. H. J. Schenning, A. F. M. Kilbinger, F. Biscarini, M. Cavallini, H. J. Cooper, P. J. Derrick, W. J. Feast, R. Lazzaroni, Ph. Leclre, L. A. McDonell, E. W. Meijer, and S. C. J. Meskers, *J. Am. Chem. Soc.* **2002**, 124, 1269–1275; c) B. W. Messmore, J. F. Hulvat, E. D. Sone, S. I. Stupp, *J. Am. Chem. Soc.* **2004**, 126, 14452–14458.
- [11] a) G. Guérin, J. Raez, I. Mannes, M. A. Winnik, *Macromolecules* **2005**, 38, 7819–7827; b) Z. Li, M. A. Hillmyer, T. P. Lodge, *Langmuir* **2006**, 22, 9409–9417.
- [12] a) Y. Zheng, Y.-Y. Won, F. S. Bates, H. T. Davis, L. E. Scriven, Y. Talmon, *J. Phys. Chem. B* **1999**, 103, 10331–10334; b) Y. He, Z. Li, P. Simone, T. P. Lodge, *J. Am. Chem. Soc.* **2006**, 128, 2745–2750; c) Y. Zheng, Y.-Y. Won, F. S. Bates, H. T. Davis, L. E. Scriven, Y. Talmon, *J. Phys. Chem. B* **2003**, 107, 3095–3097.
- [13] a) E. Lee, Z. Huang, J.-H. Ryu, M. Lee, *Chem. Eur. J.* **2008**, 14, 6957–6966; b) E. Lee, J.-K. Kim, M. Lee, *Angew. Chem.* **2008**, 120, 6475–6478; *Angew. Chem. Int. Ed.* **2008**, 47, 6375–6378.
- [14] a) E. E. Dormidontova, *Macromolecules* **2002**, 35, 987–1001; b) G. D. Smith, D. Bedrov, *J. Phys. Chem. B* **2003**, 107, 3095–3097.
- [15] J.-H. Ryu, E. Lee, Y.-b. Lim, M. Lee, *J. Am. Chem. Soc.* **2007**, 129, 4808–4814.
- [16] a) Z. Li, M. A. Hillmyer, T. P. Lodge, *Nano Lett.* **2006**, 6, 1245–1249; b) R. Oda, I. Huc, D. Danino, Y. Talmon, *Langmuir* **2000**, 16, 9759–9769.